SMiRT-12 / K. Kussmaul (Editor)
© 1993 Elsevier Science Publishers B.V. All rights reserved.

H03/5

STRESS ANALYSIS OF CONCRETE WALL DURING MOISTURE PROPAGATION

P. Majumdar, A. Gupta and A. Marchertas

Northern Illinois University, USA

1. ABSTRACT

Plane and axisymmetric stress analysis calculations are superimposed over the calculations of moisture propagation through a concrete containment wall. Temperatures and pore pressures derived by the thermal mass transport calculations are used as input loading for the stress analysis. Additional pressure loading derived from other sources or specific constraints can be imposed on these calculations as well. The stress analysis can be specified to be performed under plane stress, plane strain or axisymmetric conditions.

Finite element analysis, assuming homogeneous materials properties, is applied for the heat and mass transfer as well as for stress analysis calculations. The discretization used in moisture propagation is also utilized for stress analysis. Stress analysis in fact, is decoupled from the moisture calculations; the state of stress (and displacements are performed only at the time when output is requested in the computer program.

2. INTRODUCTION

A number of studies have been initiated to provide analytical simulation of temperature and pore pressure propagation to understand the phenomena of moisture leakage through concrete. Experimental data also exist which give information of leakage both through uncracked and cracked concrete. These data are essential in the validation of the analytical simulation.

Analytical means are also required to study the stress field of concrete walls which undergo thermal and pore pressure propagation. An analytical stress analysis computer program is thus provided to estimate the principal stresses, subject to the input of temperature and pore pressure derived from the thermal/mass transport calculation. This is accomplished to yield stress calculations at the time when output is specified. Hence, the stresses are decoupled from temperature and pore pressure calculations.

The present analysis provides the first step to estimate the crack propagation through the concrete wall. The knowledge of crack propagation is essential, because then the moisture and temperature propagation through the wall would be greatly affected. At that stage the crack prediction would interface with acceleration of moisture propagation and the analyses would become coupled.

At this time, however, moisture propagation analyses hold only to crack-free material. The stress analysis assumes the material to be homogeneous - one without cracks. Furthermore, it is based on purely elastic stress/strain relations. Analytical modifications would need to be implemented to account for cracks.

Since the analysis yields only elastic stress distributions, it yields a means of indicating trends of stresses throughout the wall and for the duration of this heating/pressure process. Boundary conditions may include temperature as well as pressure at the inside boundary; displacement constraint are also available.

3. ANALYTICAL FORMULATION

A simple element, a four-node quadrilateral element shown in Figure 1, is selected for the stress analysis. This simple element will facilitate a good approximation of the average state of stress in the element. In turn, it will also enable the establishment of a single crack within the element in the future.

The element stiffness matrix [k] and the force vector {f} are expressed by volume (V) and surface (S) integrals as $[k] = \int_V [B]^T [D] [B] \, dV$

$$\{f\} = \int_V [B]^T [D] \{\epsilon_T\} \, dV + \int_V [N]^T \begin{Bmatrix} R \\ Z \end{Bmatrix} dV + \int_S [N]^T \begin{Bmatrix} p_r \\ p_z \end{Bmatrix} dS$$

where the individual component terms of the force vector contribution correspond to thermal, body force, and pressure force, respectively. The shape functions for the element in terms of the local coordinates ξ and η are $N_1 = 0.25\,(1-\xi)\,(1-\eta)$, $N_2 = 0.25\,(1+\xi)\,(1-\eta)$, $N_3 = 0.25\,(1+\xi)\,(1+\eta)$, and $N_4 = 0.25\,(1-\xi)\,(1+\eta)$. Matrix [D] is the material property matrix which relates elastic stress to strain $\{\sigma\} = [D]\{\epsilon\}$ where for axisymmetric geometry the stress and strain components are $\{\sigma\}^T = [\sigma_r \; \sigma_z \; \sigma_{rz} \; \sigma_t]$ and $\{\epsilon\}^T = [\epsilon_r \; \epsilon_z \; \epsilon_{rz} \; \epsilon_t]$. Furthermore, the material matrix for plane stress conditions and for plane strain as well as for axisymmetric problems, respectively, are

$$[D] = \frac{E}{1-\nu^2} \begin{bmatrix} 1 & \nu & 0 & \nu \\ \nu & 1 & 0 & \nu \\ 0 & 0 & (1-\nu)/2 & 0 \\ \nu & \nu & 0 & 1 \end{bmatrix} \qquad [D] = \frac{E}{(1+\nu)(1-2\nu)} \begin{bmatrix} 1-\nu & \nu & 0 & \nu \\ \nu & 1-\nu & 0 & \nu \\ 0 & 0 & \frac{1}{2}-\nu & 0 \\ \nu & \nu & 0 & 1-\nu \end{bmatrix}$$

The [B] matrix relates the strain components to the nodal displacements as $\{\epsilon\} = [B]\{u\}$, where for axisymmetric geometry and a linear four-point quadrilateral element becomes $\{u\}^T = [u_1 \; w_1 \; u_2 \; w_2 \; u_3 \; w_3 \; u_4 \; w_4]$. By using the total strain-displacement relations

$$e_r = \frac{\partial u}{\partial r}, \qquad e_z = \frac{\partial w}{\partial z}, \qquad e_{rz} = \frac{\partial u}{\partial z} + \frac{\partial w}{\partial r}, \qquad e_t = \frac{u}{r}$$

and utilizing relationships of displacements u, w with respect to nodal displacements u_i,

$$u = \sum_{i=1}^{4} N_i \, u_i \qquad\qquad w = \sum_{i=1}^{4} N_i \, u_i$$

the expression for [B] for the four-node quadilateral element becomes

$$[B] = \begin{bmatrix} \frac{\partial N_1}{\partial r} & 0 & \frac{\partial N_2}{\partial r} & 0 & \frac{\partial N_3}{\partial r} & 0 & \frac{\partial N_4}{\partial r} & 0 \\ 0 & \frac{\partial N_1}{\partial z} & 0 & \frac{\partial N_2}{\partial z} & 0 & \frac{\partial N_3}{\partial z} & 0 & \frac{\partial N_4}{\partial z} \\ \frac{\partial N_1}{\partial z} & \frac{\partial N_1}{\partial r} & \frac{\partial N_2}{\partial z} & \frac{\partial N_2}{\partial r} & \frac{\partial N_3}{\partial z} & \frac{\partial N_3}{\partial r} & \frac{\partial N_4}{\partial z} & \frac{\partial N_4}{\partial r} \\ \frac{N_1}{r} & 0 & \frac{N_2}{r} & 0 & \frac{N_3}{r} & 0 & \frac{N_4}{r} & 0 \end{bmatrix}$$

The remaining symbols in the force vector expression are the thermal strain vector $\{\epsilon_r\}^T = \alpha\ \Delta T\ [1\ 1\ 0\ 1]$ and the r and z components of the body force (R, Z) and surface force, (p_r, p_z), respectively. Components for ΔT and (R, Z) would be comprised of temperature and pore pressure from the TEMPOR2 solution, while (p_r, p_z) would take on the imposed pressures at the boundaries of the analytical model.

4. IMPLEMENTATION OF THE COMPUTER PROGRAM

The stress analysis calculations are superimposed over the temperature/moisture calculations for the same discretization performed in the TEMPOR2 Computer Program [1]. The output of the nodal temperature and pore pressure values are used as input loading for the stress analysis. In fact, an implicit calculation of displacement and stress is performed only for the user-specified output. Consequently, the two sets of calculations are decoupled from each other.

In the plane 1-D and axisymmetric calculations of temperature and pressure, a row of 2-D four-node quadrilateral elements is used for stress simulations. Numerical four-point integration is utilized for the evaluation of element stiffness matrix and force vector. Plane stress, plane strain, or axisymmetric geometry may be specified for the stress analysis. For convenience, only a single-point integration is performed to display the element strain and stress values. Principal stresses are also calculated.

Aside from the original temperature and pore pressure acting on every node, additional pressure and temperature can be prescribed at the element boundaries. Displacement constraint may also be specified.

5. NUMERICAL ILLUSTRATION

The geometry of the 1-D illustrative example of a concrete wall is shown in fig. 2. One hundred equal-size elements are assumed for numerical calculations. Input data for thermal/moisture migration problem are shown in Table I. For stress analysis the input data are given in Table II. The thermal input at the inside boundary of the wall is taken from the paper by England et al. [2], and is reproduced in fig. 3.

The TEMPOR2 (1-D) computer calculations of temperature and pore pressure are illustrated in figs. 4 and 5, respectively. They do conform to typical output for temperature and moisture transport calculations in concrete.

All nodal displacements and plane strain and stress values are produced by the analytical solution. Because concrete is weak in tension, the maximum values of tensile stress are of primary interest. The corresponding principal stress output for a plane stress solution is given in fig. 6. It is observed that a sharp tensile stress spike exists at 11 min. after the initiation of the solution. The location of the spike is about 0.875 cm inside the wall; subsequently, the stress subsides to lower magnitudes. It may be observed that the presence of the spike is due to the largest temperature differences inside the wall, corresponding to the largest temperature gradient of the input.

The tensile stress variation with time is depicted in fig. 7. It shows that largest stress occurs during the largest input temperature gradient at the surface. A similar stress variation is shown in fig. 8, where the

pore pressure loading is incorporated. By comparing these results to those in fig. 6, it is observed, that the effect of pore pressure on the stress peak is minor, but the duration of the stress is significantly magnified.

The identical input conditions of temperature and without pore pressure are also assumed for a plane strain solution. The results are displayed in fig. 9. By comparing figs. 7 and 9, it is observed that the output of plane stress and plane strain conditions is insignificant.

6. CONCLUDING REMARKS

The computer program provides a convenient tool to calculate the state of stress in a homogeneous concrete wall which is subjected to temperature and moisture propagation. The magnitude of tensile stresses can be monitored to seek indications of crack openings.

The illustrated example showed stress below the usual tensile stress limit. However, if it is assumed that cracks exist in the original material, then any tensile stress would tend to open those cracks. Then the temperature and pore pressure propagation , which had been assumed for homogeneous material, would be altered and the original formulation would need to be changed so that the effect of cracking would be taken into account.

The numerical values of stress shown, illustrate the qualitiative variation with time and space. It is realized that more meaningful results could be accomplished when accurate values of modulus of elasticity, Poisson's ratio and coefficient of thermal expansion for concrete are utilized in the calculations. Accuracy should reflect the variation of these properties with temperature and moisture content.

Table I. Input parameters to TEMPOR2 (1-D)

NELEM	100	NTSFI	10
NPSFI	1	NTSFO	1
NPSFO	1	NTIMEH	4
Age of concrete	40 days	Volume of specimen	210 m^3
Humidity of concrete	0.95	Option for weight loss	0
Humidity of environment	0.70	Inner radius	1000 m
Initial temperature	20°C	Thermal conductivity	1.674 J/m-s-°C
Thickness of concrete	0.35 m	Permeability	10^{-11} m/s
Saturation water	100 kg/m^3	Thermal moisture flux	0.0
Weight of cement per concrete volume	300 kg/m^3	Program will be terminated at	60 min
Unit weight of concrete	2400 kg/m^3	First output at	0.0 min
Water/cement ratio	0.5	Time increment for output	1.0 min

TABLE II. Input parameters for stress analysis

Modulus of elasticity	36 MPa	Coefficient of thermal expansion	9.5×10^{-6}/°C
Poisson's ratio	0.2	Cross-sectional area	1.0 m^2

7. REFERENCES

1. Bazant, Z.P., Chern, J.C., and Thonguthai, W. 1981. "Finite Element Program for Moisture and Heat Transfer in Heated Concrete," Nuclear Engineering and Design, Vol. 68: pp. 61-70.
2. England, G.E., et al. 1991. "Influence of High Temperature on Water Content, Permeability and Pore Pressure in Concrete." SMiRT-11 Transactions, Vol. H: pp. 31-36.

ACKNOWLEDGEMENT: Part of the work described in this paper was supported by the SHIMIZU Corporation, Nuclear Reactor Division, through a subcontract of the Argonne National Laboratory.

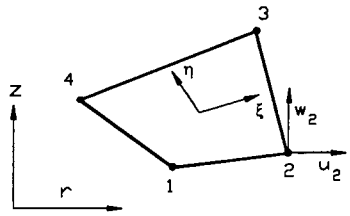

Fig. 1. Quadrilateral Element Used in Stress Analysis

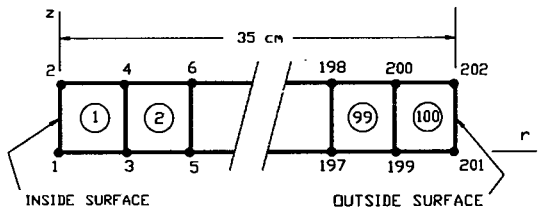

Fig. 2. Discretization of the Analytical Model

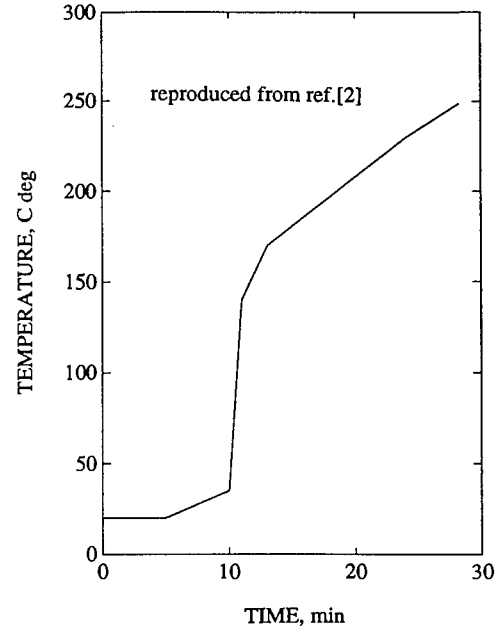

Fig. 3. Temperature input at the Inside Boundary

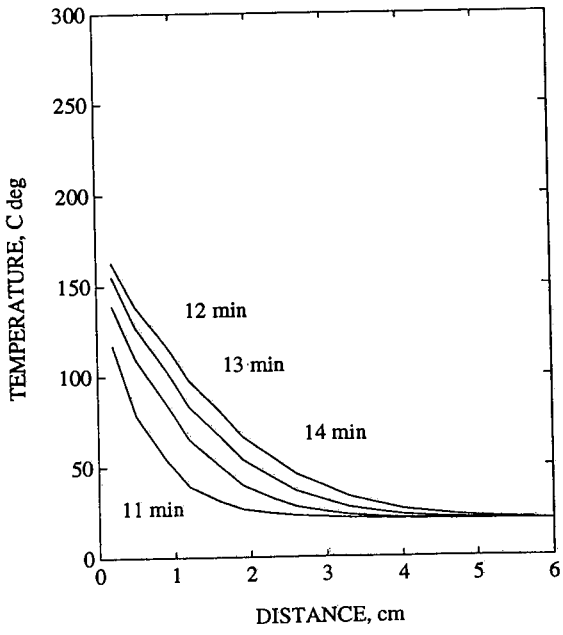

Fig. 4. Temperature Output of TEMPOR2 Program

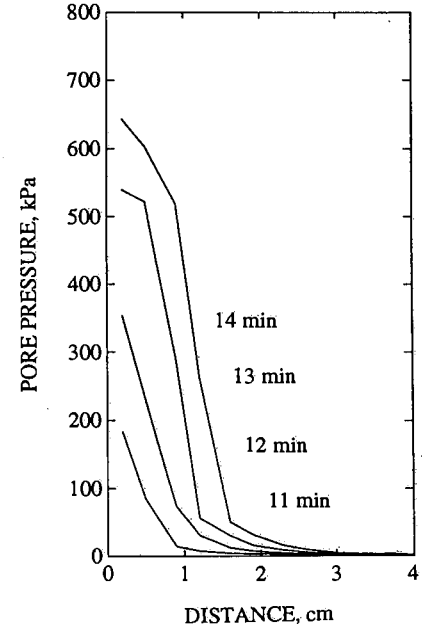

Fig. 5. Pore Pressure Output of TEMPOR2 Program

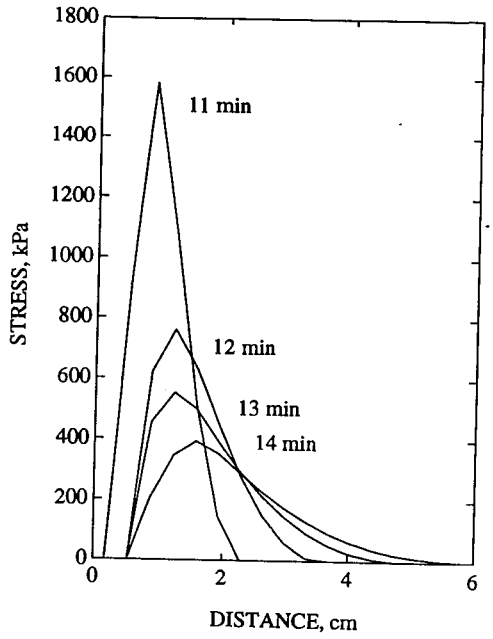

Fig. 6. Maximum Tensile Stress Distribution Under Plane Stress

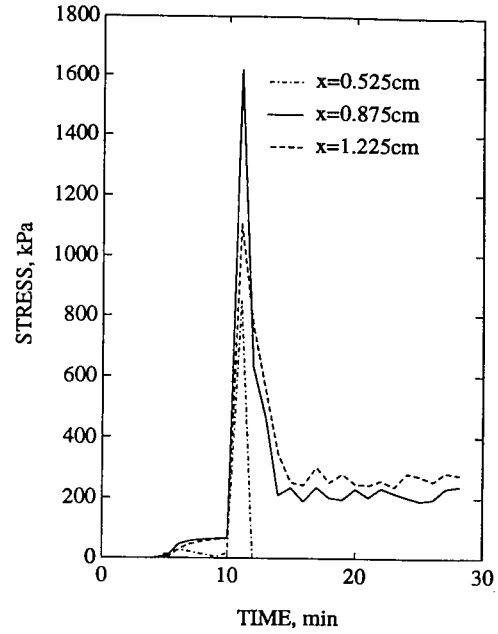

Fig. 7. Tensile Stress History At Different Locations Without Pore Pressure

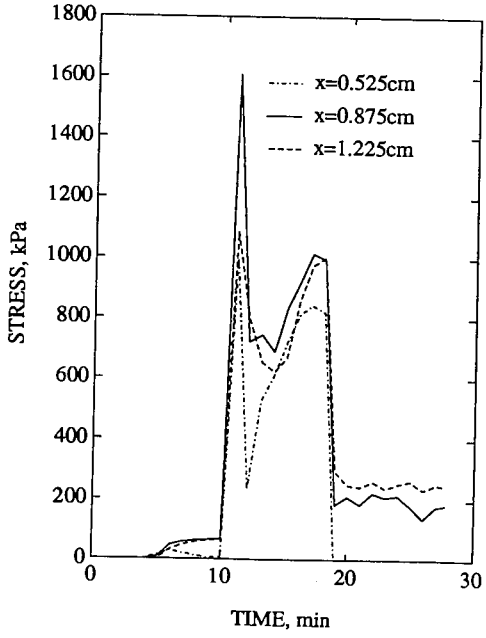

Fig. 8. Tensile Stress History Under Thermal and Pore Pressure Loading

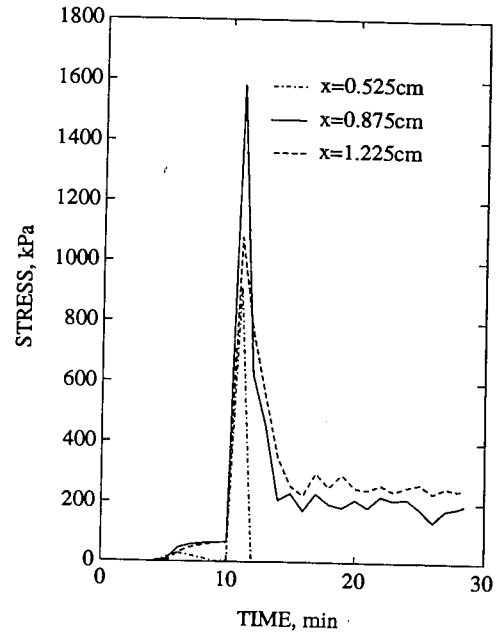

Fig. 9. Tensile Stress History Assuming Plane Strain